ELSEVIER

Journal of Power Sources 54 (1995) 301–305

JOURNAL OF POWER SOURCES

Characterization of the lithium–organic electrolyte interface containing inorganic and organic additives by in situ techniques

Yoshiharu Matsuda, Masashi Ishikawa *, Shinsuke Yoshitake, Masayuki Morita

Department of Applied Chemistry and Chemical Engineering, Faculty of Engineering, Yamaguchi University, Tokiwadai, Ube 755, Japan

Abstract

New inorganic additives, tin(II) iodide and aluminum iodide (AlI_3), improved charge/discharge cycling efficiency of a lithium (Li) electrode in propylene carbonate electrolyte containing lithium perchlorate as the electrolytic salt. The combination of different types of additive, i.e., the addition of AlI_3 together with 2-methylfuran to the electrolyte, resulted in an excellent cycling efficiency of the Li electrode. The electrochemical behavior of an Li electrolyte–organic electrolyte interface was investigated by in situ techniques such as a.c. impedance measurements and scanning vibrating electrode technique. The relation between the Li rechargeability and the interfacial behavior of the Li electrode in the organic electrolyte in the absence and the presence of the additives was discussed.

Keywords: Lithium electrodes; Organic electrolytes; Additives

1. Introduction

The optimal modification of lithium (Li) electrode–organic electrolyte interface has been considered to be important because the charge/discharge behavior of an Li electrode is much affected by the structure of the Li electrode–electrolyte interface. Recently, it has been reported that some inorganic and organic additives in the electrolytes can improve the cycling efficiency of Li electrodes in organic electrolyte systems [1–7]. In this context, we have proposed some inorganic and organic additives to improve the cycling efficiency of the Li electrode and discussed the mechanism of their addition effects [2,5–7]. The inorganic ions, such as Mg^{2+}, Zn^{2+}, In^{3+} and Ga^{3+}, would form thin layers of Li alloys at the electrode surface during cathodic deposition of Li, and the resulting thin films suppress the dendritic deposition of Li that causes the lowering of the coulombic efficiences in the charge/discharge cycles [2,7]. On the other hand, the reaction between the organic additives, such as 2-methylthiophene (2MeTp) and 2-methylfuran (2MeF), and Li would form solid–electrolyte interface (SEI) whose conductance is higher than that formed in the electrolytes without additives [3–7]. Such a surface film with high conductivity would protect Li electrode and contribute to improving the coulombic efficiency of Li in the electrochemical deposition/dissolution process [3–7].

We propose herein new inorganic additives, tin(II) iodide (SnI_2) and aluminum iodide (AlI_3), which improve the cycling efficiency of Li, and also report the synergistic effect of AlI_3 and 2MeF on the cycling efficiency. This paper describes the relation between the Li rechargeability and the interfacial behavior of the Li electrode in the organic electrolyte in the absence and the presence of the additives. The structure of the Li electrode–organic electrolyte interface was investigated by an a.c. impedance method and scanning vibrating electrode technique (SVET) [8]; the latter technique has never been used for Li-battery systems. The base system was metallic Li in propylene carbonate (PC) dissolving lithium perchlorate ($LiClO_4$).

2. Experimental

The solvent, PC (Mitsubishi Petrochemical, Battery Grade), was used as-received. The electrolytic salt, $LiClO_4$ (Ishizu Pharmaceutical, Extra Pure Grade), was dissolved in PC and its concentration was 1 M. The additives were AlI_3, SnI_2, lithium bromide (LiBr), lithium iodide (LiI), and 2MeF and were used after dehydration with conventional methods. A conventional beaker-type glass cell with three electrodes was used

* Corresponding author.

SSDI 0378-7753(94)02088-K

for charge/discharge and a.c. impedance measurements. The test electrode was a nickel (Ni) disk, whose surface area exposed to the electrolyte solution was 0.95 cm^2. The counter and the reference electrodes were an Li sheet (~25 cm^2) and an Li chip (Li/Li^+), respectively. The coulombic efficiency in the charge/discharge cycle of Li was determined by a galvanostatic deposition/dissolution technique using a Ni disk substrate. The current density for cycling was 2.0 mA cm^{-2}, and the charged electricity was 0.2 C cm^{-2}. A cutoff voltage for the discharge of the test electrode was 1.5 V versus Li/Li^+. The a.c. impedance at the Li-deposited electrode–electrolyte interface was measured by a frequency response analyzer (Solartron, 1250A). In the impedance measurement, the current density for cycling was 2.0 mA cm^{-2}, and the charged electricity was 0.15 C cm^{-2}. A cutoff voltage for discharging was 1.5 V versus Li/Li^+. The a.c. voltage of 10 mVp-p was applied to the Li-deposited Ni electrode under open-circuit voltage conditions. The frequency was scanned from 65 kHz to 1 Hz. SVET system (Hokuto Denko, HV-101) was applied to measure potential gradient profiles induced by Li ionic currents on the surface of the Li-deposited electrode during the discharge in the presence and the absence of additives. All electrochemical measurements were carried out under argon atmosphere at room temperature (20–25 °C).

3. Results and discussion

Fig. 1 shows coulombic efficiencies for charge/discharge cycling of Li in $PC/LiClO_4$ (1 M) solutions in the absence and the presence of LiBr or LiI under a constant-charge/discharge current of 2.0 mA cm^{-2}. A rest time between discharging and charging was 50 s. No obvious improvement in the cycling efficiency was observed for the system with LiBr in comparison with the efficiency in the system without additives. On the other hand, the addition of LiI (the concentration of I^- was 100 ppm or 300 ppm) improved the coulombic efficiency especially after ~10th cycle. The addition effect of LiI would be ascribed to the physical adsorption of the iodide anion on the electrode. This adsorption would inhibit an interfacial reaction, which forms low-conductive film, between Li and PC solvent on the Li surface, and hence the cycling behavior of the Li electrode would be improved. Furthermore, the reaction between the iodide anion and Li on the electrode surface may form the high-conductive LiI layer which prevents the reaction between Li and PC [9]. This process may also improve the cycling efficiency of the Li electrode.

Fig. 2 displays coulombic efficiencies for charge/discharge cycling of Li in $PC/LiClO_4$ (1 M) solutions in the absence and the presence of SnI_2, AlI_3, or AlI_3+2MeF under the constant current of 2.0 mA cm^{-2}. The rest time between discharging and charging was also 50 s. The improvement of the efficiency was observed for each additive. The efficiency increased in the order of no additive $< SnI_2 \cong AlI_3 < AlI_3 + 2MeF$ system. Both Sn and Al are well known to form Li alloys [7]. It is supposed that the thin layers of the Li alloys at the electrode surface during cathodic deposition of Li suppress the dendritic deposition of Li which causes the lowering of the coulombic efficiencies [2,7]. The iodide anion may also play an important role in the improvement of the efficiency as described above. The effect of SnI_2 was nearly equivalent to that of AlI_3. Furthermore, the positive synergistic effect of AlI_3 and 2MeF on the efficiency was observed. The SEI formed by 2MeF would also protect the Li electrode together with the Li-alloy film as well as iodides and contributes to improving the efficiency of Li in the electrochemical cycling process [5–7].

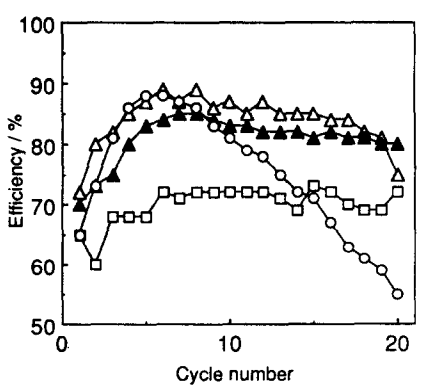

Fig. 1. Addition effects of LiI and LiBr on charge/discharge coulombic efficiency of Li in PC with $LiClO_4$ (1 M); current density: 2.0 mA cm^{-2}; charged electricity: 0.2 C cm^{-2}; rest time: 50 s. (○) no additive: (△) LiI (I^- 100 ppm); (▲) LiI (I^- 300 ppm), and (□) LiBr (Br^- 100 ppm).

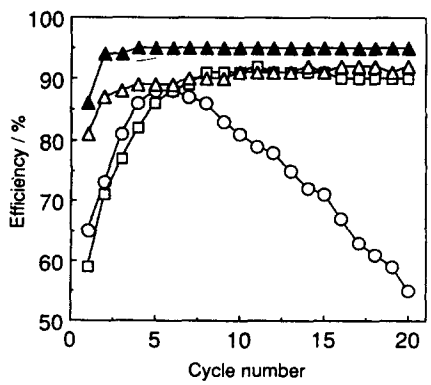

Fig. 2. Addition effects of SnI_2, AlI_3, and AlI_3+2MeF on charge/discharge coulombic efficiency of Li in PC with $LiClO_4$ (1 M); current density: 2.0 mA cm^{-2}; charged electricity: 0.2 C cm^{-2}; rest time: 50 s. (○) no additive; (□) SnI_2 (Sn^{2+} 100 ppm); (△) AlI_3 (Al^{3+} 100 ppm), and (▲) AlI_3 (Al^{3+} 100 ppm) + 2MeF (0.5 vol.%).

The electrochemical deposition of Al or Sn together with Li in the typical systems was confirmed by an atomic absorption analysis of the deposit on the Ni substrate. The charged electricity which was consumed in the deposition of Al and Sn during first charging process corresponds to 41 and 45% of the total charged electricity, respectively. It was found that the amount of Al or Sn remained on the electrode did not appreciably change even after repeating cycle (e.g., 20th cycle). Thus, the Li alloy with Al or Sn would be formed at each charge/discharge cycle.

In order to study the correlation between the cycling behavior and the interfacial structure of the Li–electrolyte interface, a.c. impedance measurements were performed in the absence and the presence of the additives. The resistive components (R) in the impedance are plotted in Fig. 3 as a function of the charge/discharge cycle number. In this experiment, a nickel plate was used as the test electrode. An increase in the interface resistance with cycling in PC/$LiClO_4$ suggests that the surface film with a high resistance grew with repeating the cycle. In our experiment, the system without additives showed the highest resistance increasing with an increase in the cycle number. The resistance decreased in the order of no additive > LiI > SnI_2 > AlI_3 ≅ AlI_3 + 2MeF. Especially, as for the systems with AlI_3, the resistances were almost constant and independent of the cycle number. This result suggests that Al formed the Li-alloy films with high conductivity at the electrode surface. On the other hand, the addition of SnI_2 caused a higher resistance than that of AlI_3 at the interface. This high resistance is undesirable for the Li cycling with high efficiency. However, the efficiency measurement with the short rest time (50 s) in Fig. 2 represented that the addition of SnI_2 resulted in an increase in the cycling efficiency of Li and this effect was almost equivalent to that of AlI_3. The inorganic ions, Al^{3+} and Sn^{2+} would form thin layers of Li alloys at the electrode surface during cathodic deposition of Li, and the resulting thin films suppress the dendritic deposition of Li that causes the lowering of the coulombic efficiencies in the charge/discharge cycles [2,7]. Because the charge/discharge cycling in Fig. 3 included the long rest time (~950 s) for impedance analysis, we suppose that the efficiency in the SnI_2 system should decrease when the charge/discharge cycle includes longer rest time than 50 s, although the addition of SnI_2 causes the formation of Li alloy films.

Fig. 4 displays coulombic efficiencies for charge/discharge cycling of Li in PC/$LiClO_4$ (1 M) solutions in the presence of SnI_2 or AlI_3 under a constant current of 2.0 mA cm^{-2} with the longer rest time between charging and discharging (950 s). The efficiency observed for the AlI_3 system (rest time 950 s) in Fig. 4 was almost equal to that observed for the AlI_3 system (rest time 50 s) in Fig. 2. However, the efficiency in the SnI_2 system (rest time 950 s) in Fig. 4 was considerably lower than that in the corresponding system (rest time 50 s) in Fig. 2. Based on these results, AlI_3 is regarded as a more practical additive than SnI_2 because AlI_3 worked effectively under representative various operating conditions.

In order to obtain the further in situ interfacial information, we applied SVET [8] for the detection of the two-dimensional distribution of ionic currents on the Li-deposited electrode surface. Fig. 5 represents schematic configuration of the in situ SVET system. A Pt wire electrode attached to a sensor probe was vibrated (80 Hz) along a vertical axis in the vicinity of a test electrode surface (the distance between the Pt electrode and the test electrode was 0.3 mm) by a piezoelectric oscillator; in our system the test electrode was a Ni plate (20 mm × 20 mm) laid on the bottom of a test cell. The other Pt wire electrode in an indiferrent probe was used to remove background noise and does not detect the ionic current in itself. We can obtain a potential gradient value, defined as a potential gap

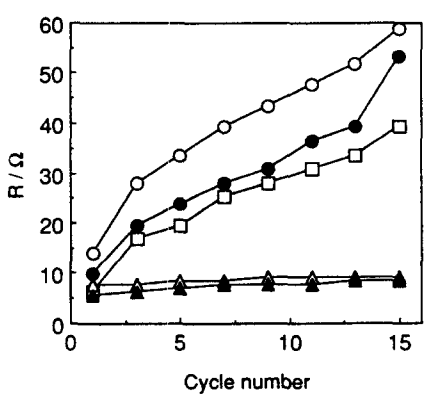

Fig. 3. Variation of R with cycle number in PC with $LiClO_4$ (1 M); electrode area: 0.95 cm^2. (○) no additive; (●) LiI (I^- 300 ppm); (□) SnI_2 (Sn^{2+} 100 ppm); (△) AlI_3 (Al^{3+} 100 ppm); and (▲) AlI_3 (Al^{3+} 100 ppm) + 2MeF (0.5 vol.%).

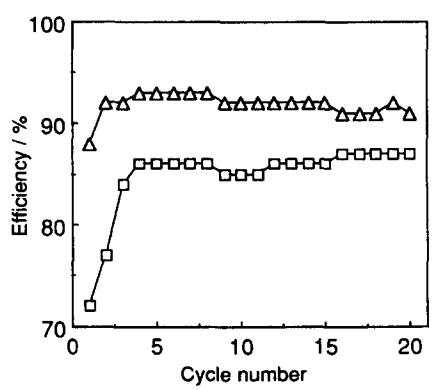

Fig. 4. Addition effects of SnI_2 and AlI_3 on charge/discharge coulombic efficiency of Li in PC with $LiClO_4$ (1 M); current density: 2.0 mA cm^{-2}; charged electricity: 0.2 C cm^{-2}; rest time: 950 s. (□) SnI_2 (Sn^{2+} 100 ppm) and (△) AlI_3 (Al^{3+} 100 ppm).

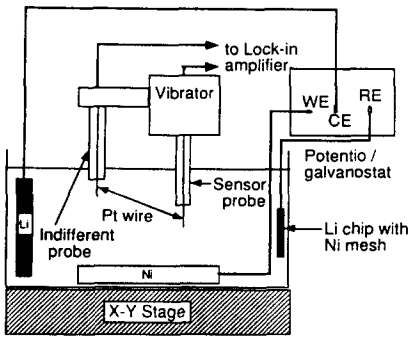

Fig. 5. Schematic configuration of the scanning vibrating electrode system.

between potentials detected by the Pt sensor electrode at the highest position and that at the lowest position during the vertical vibration of the Pt electrode. The distance between the highest and the lowest positions was 10 μm. Therefore, the potential gradient values correspond to the potential gaps between a distance of 10 μm along the vertical in the vicinity of the test electrode surface. The potential gradient would be proportional to the ionic current in the vicinity of the electrolyte/electrode interface, because the resistance of the electrolytes would be regarded as a constant value. Thus, the potential gradient value would increase with an increase in ionic current flow. In our SVET system, the positive potential gradient value corresponds to an anodic stripping current of Li while the negative value represents the cathodic plating current. The x–y stage, on which the test cell with the test electrode was mounted, was horizontally moved by a stepping motor, while both the sensor and the indifferent probes were fixed. Gathering the potential gradient values at various x–y positions, therefore, two-dimensional potential gradient map on the test electrode can be obtained. In addition, a potentiostat/galvanostat was used for the charge and the discharge of Li on the Ni test electrode. The counter and the reference electrodes were an Li sheet and an Li chip (Li/Li^+), respectively.

The potential gradient map of Li-deposited Ni electrode in $PC/LiClO_4$ (1.0 M) during discharge at 50 mV versus Li/Li^+ is shown in Fig. 6. The positive potential gradients corresponding to the anodic ionic currents were observed. However, there was a considerable irregularity of the ionic currents on the Ni electrode surface. Especially, there were a lot of sites where the potential gradient value was zero, i.e., no ionic current was at these sites, suggesting that the electrode had many inactive sites for Li stripping. On the other hand, on the Li-deposited Ni electrode in $PC/LiClO_4$ containing AlI_3 (Al^{3+} 100 ppm) and 2MeF (0.5 vol.%) during discharge at 50 mV versus Li/Li^+, the ionic currents were much higher than those in the non-additive system (Fig. 6) as shown in Fig. 7. In addition, the inactive site corresponding to zero potential gradient

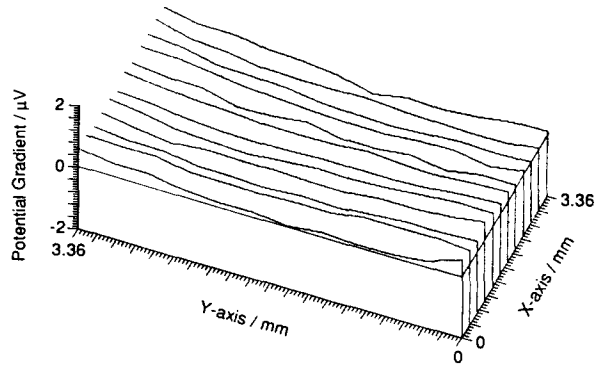

Fig. 6. Potential gradient map of Li-deposited Ni electrode in PC/$LiClO_4$ (1 M) during discharge; current density for charge: 1.0 mA cm^{-2}; charged electricity: 1.5 C cm^{-2}; discharge voltage: 50 mV vs. Li/Li^+.

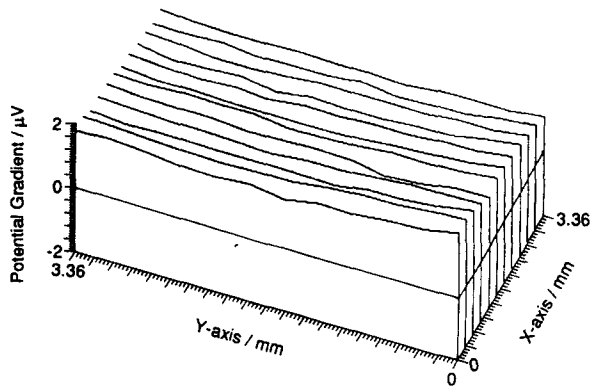

Fig. 7. Potential gradient map of Li-deposited Ni electrode in PC/$LiClO_4$ (1 M)+AlI_3 (Al^{3+} 100 ppm)+2MeF (0.5 vol.%) during discharge; current density for charge: 1.0 mA cm^{-2}; charged electricity: 1.5 C cm^{-2}, and discharge voltage: 50 mV vs. Li/Li^+.

values was not observed. This result suggests that AlI_3 and 2MeF additives provide anodic stripping of Li with a high efficiency over the electrode surface. The SVET measurements provided a clear picture of the magnitude and the distribution of the ionic currents on the electrode. We consider that this method would be a valuable tool to elucidate the interfacial phenomena involving ionic currents in Li-battery systems.

Acknowledgements

This work was financially supported by the Electric Technology Research Foundation of Chugoku. We are grateful to Hokuto Denko Corporation for the technical service.

References

[1] K.M. Abraham, *J. Power Sources, 14* (1985) 178.
[2] Y. Matsuda, M. Morita and H. Nigo, in K.M. Abraham and M. Salomon (eds.), *Primary and Secondary Lithium Batteries,*

The Electrochemical Society, Pennington, NJ, USA, 1991, p. 272.
[3] K.M. Abraham, J.S. Foos and J.L. Goldman, *J. Electrochem. Soc., 131* (1984) 2197.
[4] S. Tobishima and T. Okada, *Denki Kagaku, 53* (1985) 742.
[5] Y. Matsuda, H. Hayashida and M. Morita, in J.P. Gabano and Z. Takehara (eds.), *Primary and Secondary Ambient Temperature Lithium Batteries,* The Electrochemical Society, Pennington, NJ, USA, 1988, p. 610.
[6] M. Morita, S. Aokia and Y. Matsuda, *Electrochim. Acta, 37* (1992) 119.
[7] Y. Matsuda, *J. Power Sources, 43/44* (1993) 1.
[8] H.S. Isaacs and Y. Ishikawa, in R. Baboian (ed.), *Electrochemical Techniques for Corrosion Engineering,* National Association Corrosion Engineers, Houston, TX, USA, 1986, p. 17.
[9] K. Shahi, J.B. Wagner and B.B. Owens, in J.-P. Gabano (ed.), *Lithium Batteries,* Academic Press, London, 1983, p. 418.